Vol. **125** (2014) *ACTA PHYSICA POLONICA A* No. 2

Proceedings of the 3rd International Congress APMAS2013, April 24–28, 2013, Antalya, Turkey

The Effect of Temperature on Grain Size of SnO_2 Nanoparticles Synthesized by Sol–Gel Method

H. Köse[a,*], A.O. Aydin[a] and H. Akbulut[b]

[a]Department of Chemistry, Arts and Sciences Faculty, Sakarya University, 54187, Sakarya, Turkey
[b]Department of Metallurgy and Material Engineering, Engineering Faculty, Sakarya University
54187, Sakarya, Turkey

Tin dioxide nanoparticles were synthesized by sol–gel method and calcined at different temperatures in the range 350–750 °C. The SnO_2 precursor solution was prepared from $SnCl_2 \cdot 2H_2O$ (tin (II) chloride dihydrate), and chloride ions were removed from the solution before the sol–gel synthesis was applied. SnO_2 powders were characterized by thermal analyses, X-ray diffraction, field emission gun-scanning electron microscopy, and energy dispersive X-ray spectroscopy, and grain size of nanoparticles were determined by using the Debye–Scherrer formula.

DOI: 10.12693/APhysPolA.125.345

PACS: 81.07.Wx, 81.20.Fw, 81.20.Ev

1. Introduction

Tin dioxide (SnO_2), cassiterite structure, is a typical wide band gap n-type semiconductor (3.6 eV) and one of the most widely used semiconductor oxides due to its chemical and mechanical stabilities. SnO_2 is a non-stoichiometric structure, and its conductivity mainly originates from the oxygen vacancies [1]. The electrical and chemical properties of SnO_2 have been extensively studied because of its application as transparent electrodes for solar cells, liquid crystal displays; antistatic coatings and gas sensors; anodes for lithium ion batteries, transistors, catalyst supports; nano and ultrafiltration membranes and anticorrosion coatings [2]. Recently tin oxide-based materials have received considerable attention as promising anode materials for Li-ion batteries due to their high theoretical capacity with 1498 mAh g^{-1} [3]. Previous reports demonstrated that nanomaterials could greatly improve electrochemical performances by nanometer size effects [4].

A variety of techniques have been used to synthesize oxide nanoparticles, including sol–gel [3], hydrothermal [5], solvothermal [2], precipitation [6], spray pyrolysis [7] and thermal decomposition techniques [8]. Among these techniques, the sol–gel method attracts the most attention because of several advantages, such as excellent homogeneity, ease of controlling the doping level, ability to coat large areas and complex shapes, simple equipment requirements and low-cost processing [1].

In this study, SnO_2 nanoparticles were synthesized by sol–gel method and calcined at different temperatures in the range of 350–750 °C. It was aimed to develop the experimental parameters for producing nanosized chloride free SnO_2 particles prepared from $SnCl_2 \cdot 2H_2O$ (tin(II) chloride dihydrate) for possible application in the sensors and Li-ion battery electrodes. It was targeted to reveal the relationships between the microstructural change and the crystal structure with the calcination temperature of nano-SnO_2.

2. Experimental

The SnO_2 precursor sols were prepared by sol–gel method after removing chloride ions (Cl^-) of $SnCl_2 \cdot 2H_2O$ precursor solution. All chemicals were of analytical grade and were used without further purification. For this process, firstly, 10.0 mmol $SnCl_2 \cdot 2H_2O$ was dissolved in deionized water and then for removing of chloride ions from tin solution, a stoichiometric ratio of NH_3 (25%) solution was added. After the precipitation of tin as hydroxide ($Sn(OH)_n$, $n = 2$ or 4), the solid was filtered and washed with diluted NH_3 solution. The final precipitate was dissolved in glacial acetic acid, and then ethylene glycol was added to solution in order to form complex with tin cation. The stirring was continued from 50 °C to 80 °C until the acetic acid was removed from the obtained sol and at the end of stirring; gels were obtained and dried in an oven at 150 °C in air. Finally, precalcination step was performed on dried gels at 300 °C, and samples were calcined in the range of 350–750 °C in air at a heating rate of 2 °C/min and held at the same temperature for 2 h. Produced SnO_2 powder samples were coded as A, B, C, D, and E for the applied calcination temperatures of 350, 450, 550, 650, and 750 °C, respectively.

Synthesized powder morphologies were analyzed with field emission gum-scanning electron microscopy (FEG-SEM) (FEI QUANTA FEG 450). The composition of the products was determined by energy dispersive X-ray spectroscopy (EDS) attached to the SEM (JEOL-JSM 6060LV). The working conditions for EDS analysis include an accelerating voltage of 15 kV, a beam current of 5 nA, a working distance of 15 mm, and a life time of 60 s for each run. XRD analysis was performed with X-ray diffractometer (Rigaku D/MAX/2200/PC model device) using Cu K_α radiation ($\lambda = 1.54050$ Å) with 1°/min scanning speed using a grazing angle of 5°. The solid was also characterized with differential thermal and gravimet-

---

*corresponding author; e-mail: hkose@sakarya.edu.tr ric analyses (TGA/DTA) (SDT Q600 model of TA) to determine endo- and exothermic events that might take place during the thermal treatment. Analyses were carried out in dry air atmosphere (100 mL/min flow) and heating rate of 10 °C/min with Al_2O_3 as reference material from 25 °C to 1000 °C.

3. Results and discussion

To determine the range of calcination temperature, thermal analysis was performed on the solid sample obtained from the SnO_2 precursor gel. Figure 1a shows the TGA/DTA curves of solid sample. On the TGA curve, the weight loss about 58% below 225 °C is due to removal of adsorbed water, physisorbed acetic acid and free ethylene glycol that cannot be removed during the thermal treatment and associated with endothermic peak on the DTA curve. The second weight loss (12%) at 375 °C on TGA curve formed the broad endothermic peak on the DTA curve. It may correspond to removing chemically bonded ethoxy groups from the structure by decomposition. From 420 °C, no weight loss was observed because of stable SnO_2 structure and DTA peak may be associated with material crystallization [9].

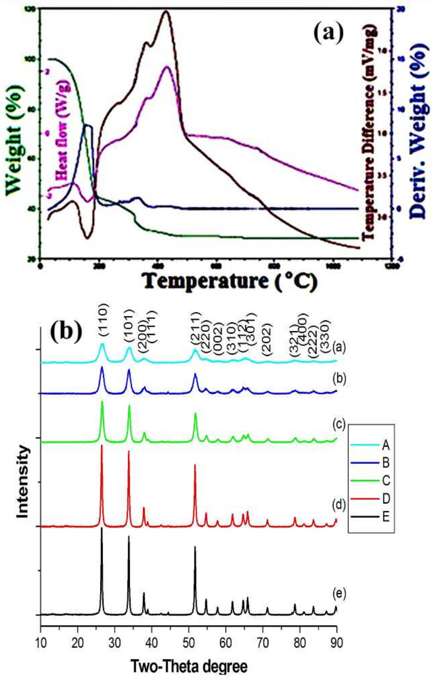

Fig. 1. (a) TGA/DTA curves corresponding to solid sample obtained from SnO_2 gel, and (b) XRD analyses of SnO_2 samples of A, B, C, D, and E.

XRD analysis was performed to investigate the crystal structure of powders. In Fig. 1b, XRD results show that there is no significant preferential nucleation and growth by changing the calcination temperature. The sharp and narrow diffraction peaks are observed at high temperatures of 650 °C and 750 °C for sample D and E, respectively. This result indicated that the particles have grown, and the crystal quality has been improved according to lower temperature calcined samples of A, B, and C [10]. It can be clearly seen that the intensity of diffraction peaks reduce with low calcination temperature, especially for the sample A. The produced phase is mainly a cassiterite type of SnO_2 (JCPDS, 00-041-1445) [3]. The strongest peak for each case is the (110) plane and the peak of SnO_2 indicated the broadest diffraction (110) peak suggesting that the nanoparticles are very small in size. The similar effect of decreasing particle size on the peak broadening in tin oxide and tin oxide based nanocomposite materials was also proven by Lian et al. [11].

Grain size of SnO_2 particles obtained from sols. TABLE

Sample	Calcination temperature	Lattice parameters [Å]	Grain size [nm]
A	350 °C	$a_{110} = b = 4.6971$ $c_{101-110} = 3.1984$	15
B	450 °C	$a_{110} = b = 4.7456$ $c_{101-110} = 3.1808$	17
C	550 °C	$a_{110} = b = 4.7388$ $c_{101-110} = 3.1776$	22
D	650 °C	$a_{110} = b = 4.7530$ $c_{101-110} = 3.1946$	36
E	750 °C	$a_{110} = b = 4.7562$ $c_{101-110} = 3.1908$	41

Standard value $a = 4.7403$ and $c = 3.1885$ (JCPDS, 00-041-1445)

Scherrer's formula (Eq. (1)) was used to determine the grain size of the SnO_2 samples by using XRD data. As can be seen from Table, the grain size increased with increase of the calcination temperature [1]. For the sample A minimum grain size was observed, and maximum grain size was obtained from the sample E which was calcined at 750 °C

$$D = \frac{K\lambda}{\beta \cos\theta}. \tag{1}$$

In this formula, K is the shape factor, D is the mean grain size of crystalline structure. λ is X-ray wavelength, β is the full width at half maximum (FWHM) or integral breadth of XRD peak, and θ is the Bragg angle. In Table, calculated grain size of samples by Scherrer's formula and lattice parameters can be seen. For the tetragonal structure, the lattice parameters can be calculated by Eq. (2) where h, k, and l are all integers, (hkl) is the lattice plane index, and a and c are lattice constants

$$\frac{1}{d_{hkl}^2} = \frac{h^2 + k^2}{a^2} + \frac{l^2}{c^2}. \tag{2}$$

For a real crystal, the calculated values of a and c are the same based on different crystal planes. However, the presence of a large number of vacant lattice sites and local lattice disorders may lead to serious reduction in the intensity (or the nearly disappearance) of the XRD peaks of the corresponding lattice plane as the sample A. There are a large number of vacancies of oxygen, vacancy clusters, and local lattice disorders, which lead to an increase in c and decrease in a and the volume of the unit cell [10], as can be seen from the values of the sample A in Table.

FEG-SEM micrographs of SnO_2 powders obtained from prepared sols are given in Fig. 2a. As can be seen from FEG-SEM image of sample A, the SnO_2 powders calcined at 350 °C showed very fine grain size of SnO_2 with spherical particles. Sample B also showed homogeneous and spherical nanosized particles for the calcination temperature of 450 °C and sample C showed similar morphology with finer particles, but agglomeration began to appear in some locations. After applying higher calcination temperatures of 650 and 750 °C, for sample D and E, particles became equiaxed coarser grains with homogeneous distribution and agglomeration can be observed. As a result, FEG-SEM images of SnO_2 samples clearly indicated that the grain size of SnO_2 powders increased with increasing in the calcination temperature and the images showed compatible results with XRD analyses and Scherrer's formula calculations.

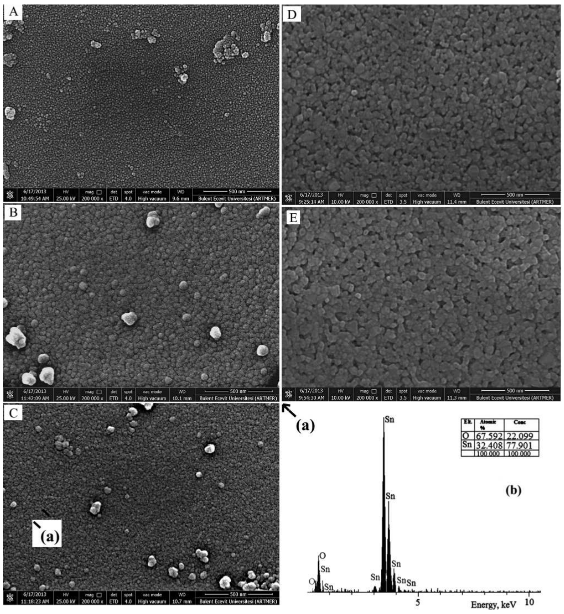

Fig. 2. (a) FEG-SEM images of SnO_2 powder samples of A, B, C, D and E, (b) EDS analysis of sample A.

In Fig. 2b, EDS analysis was taken from SnO_2 sample of A that was synthesized at the lowest calcination temperature (350 °C) to prove that no chloride ion was observed when the calcination temperature was low for the synthesis of SnO_2 nanoparticles with this method. Various precursors were used to perform the sol–gel method, such as metal alkoxides or salts. Starting from tin chlorides ($SnCl_4$ or $SnCl_2$) for obtaining SnO_2 is generally preferred because they are suitable precursor to perform and their cost is very low, but the chlorine ions are very difficult to remove and the residual chlorine ions often affect the surface and electrical properties, causing agglomeration among particles and leading to higher sintering temperatures [12]. Because of preventing undesired chloride ion we studied to remove chloride ions from the sol and EDS analysis confirmed that Cl^- anions were completely removed from sol, additionally the atomic percentage of Sn and O are suitable with the SnO_2 structure.

4. Conclusions

SnO_2 nanoparticles were synthesized with sol–gel method at different calcination temperatures from 350 °C to 750 °C. Synthesized nanoparticles were characterized by XRD, FEG-SEM, EDS and thermal analyses were performed for solid sample of SnO_2 precursor. Sol–gel method was applied with removing the chloride ion of precursor. EDS analysis shows that chloride anions were completely removed from sol. XRD analysis, lattice parameters, and grain sizes yielded coherent results. With the increase in the calcination temperature, the grain size has increased, and the crystallinity has been improved. The smallest grain size obtained from SnO_2 sample calcined at 350 °C (15 nm), and calcination temperature of 750 °C resulted in obtaining maximum grain size (41 nm). FEG-SEM images confirmed XRD results by indicating agglomeration and coarsening on spherical nanoparticles at higher temperatures. The results show that sample A, which has a large number of vacant lattice sites and minimum grain size, can be efficiently used for Li-ion battery applications, since fine nano grains provide improved charge/discharge ability associated with mesoporous structure.

Acknowledgments

This work is supported by the Scientific and Technological Research Council of Turkey (TÜBİTAK) under the contract number 109M464. The authors thank the TÜBİTAK MAG workers for their financial support.

References

[1] X. Zhong, B. Yang, X. Zhang, J. Jia, G. Yi, *Particuology* **10**, 365 (2012).

[2] G. Du, C. Zhong, P. Zhang, Z. Guo, Z. Chen, H. Liu, *Electrochim. Acta* **55**, 2582 (2010).

[3] H. Köse, A.O. Aydin, H. Akbulut, *Appl. Surf. Sci.* **275**, 160 (2013).

[4] X.M. Yin, C.C. Li, M. Zhang, Q.Y. Hao, S. Liu, L.B. Chen, T.H. Wang, *J. Phys. Chem. C* **114**, 8084 (2010).

[5] J. Zhu, D. Wang, L. Wang, X. Lang, W. You, *Electrochim. Acta* **91**, 323 (2013).

[6] M.-H. Xu, F.-S. Cai, J. Yin, Z.-H. Yuan, L.-J. Bie, *Sensors Actuat. B* **145**, 875 (2010).

[7] L. Yuan, Z.P. Guo, K. Konstantinov, J.Z. Wang, H.K. Liu, *Electrochim. Acta* **51**, 3680 (2006).

[8] A.I. del Río, J. Fernández, J. Molina, J. Bonastre, F. Cases, *Electrochim. Acta* **55**, 7282 (2010).

[9] H.A. Ávila, J.E. Rodríguez-Páez, *J. Non-Cryst. Solids* **355**, 885 (2009).

[10] K.N. Yu, Y. Xiong, Y. Liu, C. Xiong, *Phys. Rev. B* **55**, 2666 (1997).

[11] P. Lian, X. Zhu, S. Liang, Z. Li, W. Yang, H. Wang, *Electrochim. Acta* **56**, 4532 (2011).

[12] J. Zhang, L. Gao, *J. Solid State Chem.* **177**, 1425 (2004).